Science Bulletin 69 (2024) 2974–2977

Contents lists available at ScienceDirect

Science Bulletin

journal homepage: www.elsevier.com/locate/scib

Short Communication

Spin dynamics of the E_8 particles

Xiao Wang [a], Konrad Puzniak [b,c], Karin Schmalzl [d], Christian Balz [e], Masaaki Matsuda [f], Akira Okutani [g], Masayuki Hagiwara [g], Jie Ma [a,h,i,*], Jianda Wu [a,h,j,*], Bella Lake [b,c,*]

[a] Tsung-Dao Lee Institute, Shanghai Jiao Tong University, Shanghai 201210, China
[b] Helmholtz-Zentrum Berlin für Materialien und Energie GmbH, Berlin D-14109, Germany
[c] Institut für Festkö rperphysik, Technische Universität Berlin, Berlin D-10623, Germany
[d] Jülich Centre for Neutron Science JCNS, Forschungszentrum Jülich GmbH, Outstation at ILL, Grenoble 38042, France
[e] ISIS Neutron and Muon Source, STFC Rutherford Appleton Laboratory, Didcot OX11 0QX, UK
[f] Neutron Scattering Division, Oak Ridge National Laboratory, Oak Ridge 37831, USA
[g] Center for Advanced High Magnetic Field Science, Graduate School of Science, Osaka University, Osaka 560-0043, Japan
[h] School of Physics & Astronomy, Shanghai Jiao Tong University, Shanghai 200240, China
[i] Collaborative Innovation Center of Advanced Microstructures, Nanjing University, Nanjing 210093, China
[j] Shanghai Branch, Hefei National Laboratory, Shanghai 201315, China

ARTICLE INFO

Article history:
Received 5 May 2024
Received in revised form 18 July 2024
Accepted 24 July 2024
Available online 26 July 2024

Unlike the classical phase transition driven by thermal fluctuations, the quantum phase transition arises at zero temperature when the system is tuned by a non-thermal parameter [1]. For a continuous quantum phase transition, novel physics with higher symmetry may emerge at the quantum critical point (QCP). As the system is driven away from the QCP with a relevant perturbation, exotic physics may further emerge due to the strong renormalization of the almost infinite low-lying excitations [2]. The transverse-field Ising chain (TFIC) is a paradigmatic model [1–3]: when an Ising chain is tuned to its QCP by a magnetic field applied transverse to its Ising anisotropy, a central charge 1/2 conformal field theory emerges with corresponding scaling exponents falling into the class of Ising universality (Fig. 1) [3,4]. Surprisingly, when it is further perturbed by a longitudinal field parallel to the Ising direction, the quantum E_8 integrable model emerges — a massive relativistic quantum field theory containing eight massive E_8 particles (Table S1 online). The physics of the model could be described by the scattering of the E_8 particles as the maximal exceptional Lie E_8 algebra [2,5,6]. Hence, exploring quantum E_8 field theory can extend the frontier of quantum statistical field theory, and may even inspire the studies in high-energy physics.

Two conditions need to be satisfied for experimental observation of exotic E_8 physics: Accessing the Ising universality and the presence of a small perturbation field along the Ising direction. An inelastic neutron scattering (INS) experiment on the ferromagnetic chain compound $CoNb_2O_6$ provided evidence of the existence of the lightest two E_8 particles whose mass ratio was given by the Golden ratio [7]. However, an apparent deviation was presented in the spectrum continuum region between the terahertz experiment [8,9] and the analytical result [6], which implies more efforts are needed for confirming the existence of the E_8 physics in the material $CoNb_2O_6$ [10]. The quasi-1D Heisenberg-Ising antiferromagnet (AFM) $BaCo_2V_2O_8$ is believed to be another E_8 candidate [11–14]. Although all E_8 particles were found by INS [5], the measurement was confined to only the AFM zone center where several combinations of the E_8 particles and zone folding were also observed. Therefore, a full investigation of the relativistic dispersion of the E_8 particles in the whole Brillouin zone is necessary. In this work, we combine and compare experimental, analytical, and numerical approaches for the lightest three branches of excitations and unambiguously demonstrate the E_8-particles in $BaCo_2V_2O_8$.

$BaCo_2V_2O_8$, has space group is $I41/acd$ (No. 142) with the lattice constants of $a = b = 12.40$ Å and $c = 8.375$ Å [11]. The magnetic Co^{2+} ions ($S_{eff} = 1/2$) are arranged in edge-sharing CoO_6 octahedra forming 4-fold screw chains along the c-axis (inset of Fig. 1). The Co^{2+} ions are coupled by Heisenberg-Ising AFM interactions where the Ising axis is the c-axis, while weak interchain interactions give rise to long-range magnetic order below Neél temperature, $T_N = 5.5$ K. Under an external transverse magnetic field perpendicular to the spin direction (e.g., parallel to the b-axis), a three-dimensional (3D) quantum phase transition occurs at the magnetic field, $\mu_0 H_{\perp}^{c,3D} \approx 10.3$ T (Fig. 1) as the spins flop from the c- to a-axes

* Corresponding authors.
E-mail addresses: jma3@sjtu.edu.cn (J. Ma), wujd@sjtu.edu.cn (J. Wu), bella.lake@helmholtz-berlin.de (B. Lake).

https://doi.org/10.1016/j.scib.2024.07.040
2095-9273/

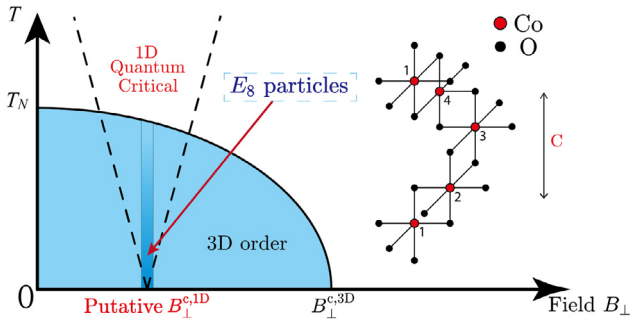

Fig. 1. (Color online) Schematic phase diagram of $BaCo_2V_2O_8$ in a transverse magnetic field. The light and deep blue indicates the AFM phase and the E_8-particle location around the 1D QCP, respectively. The inset shows one of the CoO_6 screw chains.

[5,11]. Meanwhile, the one-dimensional (1D) quantum phase transition was also discovered at $\mu_0 H_\perp^{c,1D}$ = 4.7 T [5] and lied hidden within the dome of the 3D magnetic order which provided the (staggered) longitudinal magnetic field for the E_8 quantum particles.

The INS experiment was performed using the LET neutron time-of-flight spectrometer at T = 0.3 K and $\mu_0 H//b = \mu_0 H^{c,1D}$ (= 4.7 T). Fig. 2a presents the excitation spectrum along the chain, (0, 0, L). A series of constant-momentum and energy scans were measured over wavevector Q = (0,0,1.5) to (0,0,2.5) and the energy from E = 0 to 5 meV on the IN12 triple-axis spectrometer at T = 1.5 K ($\ll T_N$) and $\mu_0 H$ = 4.7 T. Fig. 2e presented the combined into an energy-wavevector map.

According to theory, the ratios of the energies of the eight E_8-particles have precise values given in Table S1 (online). Fig. 2b shows the energy scans through the LET and IN12 datasets at Q = (0, 0, 2). As the first peak is at 1.26 meV, the theoretically expected peak positions are obtained by multiplying the E_8-particle ratios by 1.26 meV. The first three peaks in the LET and IN12 experimental data found by fitting Gaussians (observed at m_1 = 1.26, m_2 = 2.04, m_3 = 2.52 meV and at m_1 = 1.26, m_2 = 2.05, m_3 = 2.49 meV, respectively) clearly lie at the expected positions of the first three E_8 peaks. Furthermore, it should be noted that the multi-particle threshold $2m_1$ is almost the same as that with $m_3 \approx 1.99m_1$ and a zone-folding peak is close to m_2 at 1.98 meV (indicated by F_0 along [0,0,L]). Another zone-folding peak lies at 2.75 meV (indicated by F1). The fourth E_8 excitation at m_4 = 3.04 meV is very weak, while the feature at 3.30 meV is the lower boundary of the $m_1 + m_2$ multi-particle continuum. At higher energies, it is difficult to distinguish the E_8 peaks due to overlapping continua and zone-folding modes.

As high-precision data over a wide range of wavevectors were collected, we now have the opportunity to observe the behavior of the E_8-particles as well as the other excitations with a function of wavevector and energy. Returning to the energy-wavevector plots in Fig. 2a, e, the three lowest E_8 excitations clearly form dispersive modes with parabolic curvature and a minimum at Q = (0,0,2). The zone-folding modes are now easily identified, such as the dispersive excitations which have minima at the incommensurate wavevectors (0,0,1.875) and (0,0,2.15) at E=1.9 meV and overlap with m_2 at (0,0,2). Due to the multi-particle continua and overlapping modes, broad diffuse scattering is observed above 3 meV.

We performed state-of-the-art theoretical calculations of the spin dynamic structure factor (DSF) directly from quantum E_8 integrable field theory [6]. The analytical result for the dispersion of the lightest three E_8 particles is shown in Fig. 2c. iTEBD simulations were presented in Fig. 2d. These simulations take account of the screw chain structure, which gives rise to the zone folding effects and intensity modulations resulting in a spectrum similar as the actual experiment result, Fig. 2e.

The E_8-particle dispersions are expected to follow the theoretical expression:

$$\frac{E_i^2}{\Delta_1^2} = \frac{\Delta_i^2}{\Delta_1^2} + \frac{p_i^2}{(\Delta_1/c)^2} = \frac{\Delta_i^2}{\Delta_1^2} + \left(\frac{\hbar(L-2)\pi/2d}{m_1 c}\right)^2, \quad (1)$$

where $p_i = \hbar(L-2)\pi/2d$ is the momentum transfer at Q = (0,0,2) and d = 8.4192/4 = 2.105 is the nearest neighbor distance between Co^{2+} ions projected onto the chain direction. c = (1.441 ± 0.096) × 10^3 m/s, is the "speed of light" of the real material by from fitting the three lowest energy commensurate modes of the iTEBD simulation (dashed red lines in Fig. 2d) simultaneously with Eq. (1). For the IN12 data, the fitted dispersions (red lines in Fig. 2e) show good agreement with the experiment yielding $c \approx$ (1.643 ± 0.041) × 10^3 m/s, while the LET data presents $c \approx$ (1.794 ± 0.008) × 10^3 m/s. The speed of light from both experimental data and numerical simulations exhibits agreement with each other.

Comparing experimental, analytical, and numerical data with constant-momentum and energy scans (Fig. 2f, g), both analytical and iTEBD data show excellent agreement with the experimental data. There is about 1% deviation in momentum for the peak position corresponding to 1% m_1 energy shift. This possibly is from the transverse field applied in the experiment which is slightly smaller than the exact critical field, and hence, slightly heavier E_8 particles and a slightly larger minimum gap m_1 are implied. A 1% m_1 upward shift corresponds to about 0.1 to 0.2 T downward shift of the critical field whose value lies in the range of the putative QCP (4.7 ± 0.3) T identified by NMR [5]. Thus, the true critical field is considered to be (4.8 ± 0.2) T [9,14].

The quasi-1D antiferromagnet $BaCo_2V_2O_8$ is a remarkably important material in the field of quantum magnetism with unique properties: Ising-like anisotropy, large intrachain versus weak but non-negligible interchain interactions, an anisotropic g-tensor producing easy-axis anisotropy, and effective staggered fields under the application of an external magnetic field. Combining the INS experiments, theoretical, and numerical iTEBD simulations, we precisely studied the E_8 excitation spectrum at the 1D quantum critical point of B_c^{1D} = 4.7 T. The observed dispersion of the first three E_8 particles and several multi-particles modes provided smoking gun signatures for exploring quantum E_8 physics in other strongly correlated materials.

Conflict of interest

The authors declare that they have no conflict of interest.

Acknowledgments

This work was supported by the National Natural Science Foundation of China (U2032213 (J. M.), 12274288 (X. W. and J. W.)), the Innovation Program for Quantum Science and Technology (2021ZD0301900 (X. W. and J. W.), 2022YFA1402702 (J. M.)), the Natural Science Foundation of Shanghai (20ZR1428400), Shanghai Pujiang Program (20PJ1408100 (X.W. and J.W.)), and Grants-in-Aid for Scientific Research (25220803 and 24244059) from MEXT. The authors would like to thank ISIS Neutron and Muon Source, the STFC Rutherford Appleton Laboratory, and the Institut Laue-Langevin facilities for the allocation of inelastic neutron scattering beamtime. The cold neutron multi-chopper spectrometer (LET, ISIS) data (https://doi.org/10.5286/ISIS.E.RB2210086) were reduced using Mantid and were analyzed using the Horace-MATLAB software package.

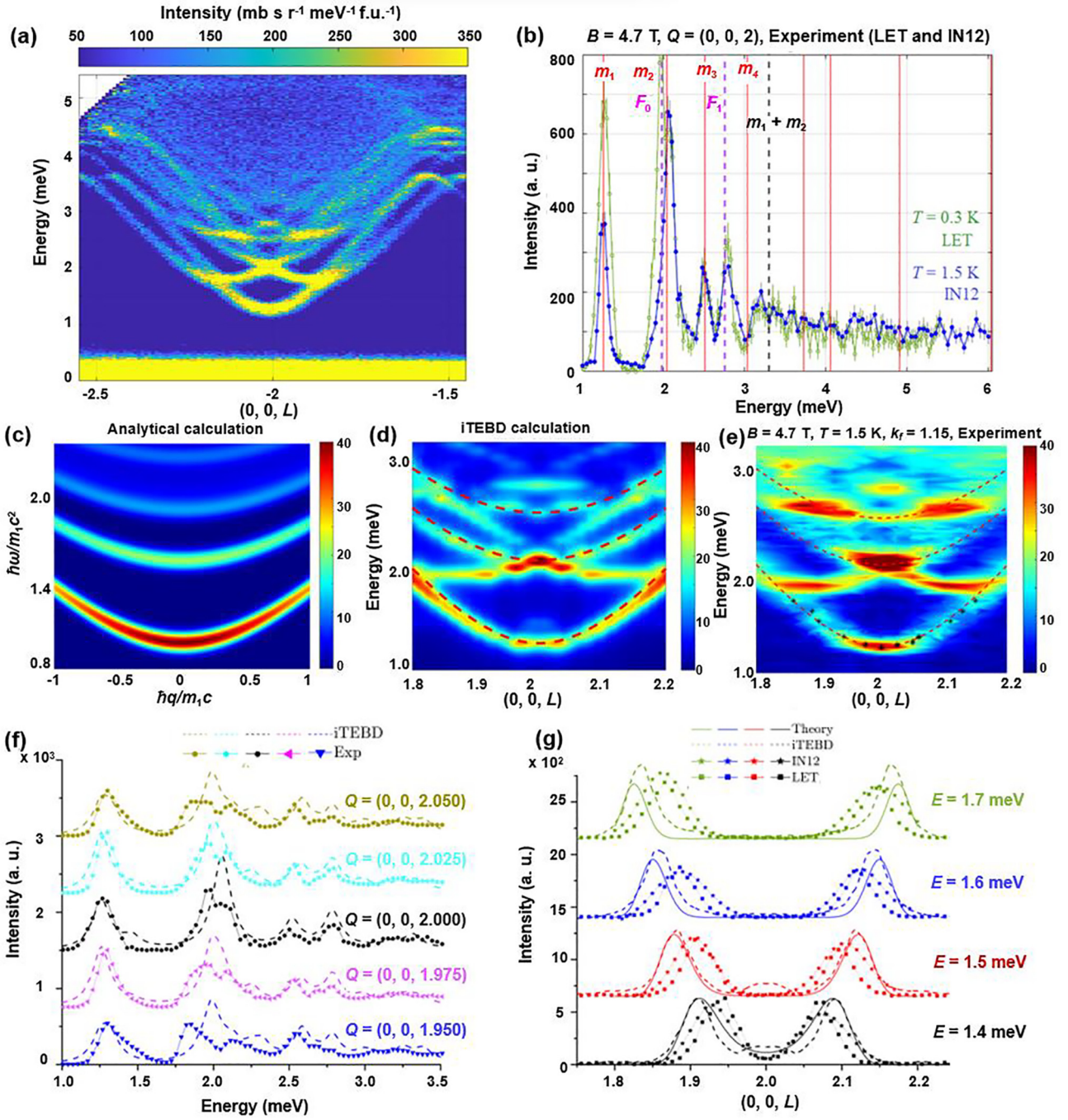

Fig. 2. (Color online) The INS spectrum, theoretical, and numerical iTEBD simulations of $BaCo_2V_2O_8$ at QCP. (a) The INS spectra under a transverse magnetic field, $\mu_0 H_\perp^{1D}$ = 4.7 T at T = 0.3 K using the LET spectrometer. The data are displayed in absolute units as a function of wavevector Q = (0,0,L) and energy, for neutron incident energy E_i = 6 meV (integration range: $-1.0 \le H \le 1.0$ & $-2 \le K \le 2$). (b) Energy scans measured at the wavevector Q = (0,0,2) on LET and IN12, with the theoretically predicted energies of the first E_8 excitations indicated by the red solid lines. Identified peaks are labelled m_n (single E_8 excitations), $m_n + m_m$ (multi-E_8 excitations) and F_n (zone-folding peaks). (c) Analytical calculation of dispersion of three lightest E_8 particles. (d) Numerical simulation of dispersion using the iTEBD method (Eq. (S4) online). The dashed lines illustrate dispersions of the three lightest E_8 particles given by Eq. (1). (e) Energy-wavevector map of the magnetic excitations constructed from constant-energy and constant-wavevector scans measured on the IN12 spectrometer at $\mu_0 H_\perp^{1D}$ = 4.7 T and T = 1.5 K. The black symbols are the peak positions extracted from fitting the individual scans, and the dashed lines are the simulated dispersions of the lowest three E_8 particles by using Eq. (1). (f, g) Comparison of DSF results between the iTEBD data, the analytical data, and the experimental IN12 and LET data for constant-moment and energy cuts, respectively. The presented LET experimental constant momentum and constant energy cuts are shifted by an offset of 0.004 r.l.u (relative lattice unit) from experimental conditions. All DSF intensities are normalized up to the maximum intensity of experimental data.

Author contributions

Jianda Wu, Jie Ma, and Bella Lake conceived and coordinated the project. Masaaki Matsuda, Akira Okutani, Masayuki Hagiwara, Jie Ma, Konrad Puzniak, and Bella Lake synthesized the crystals. Jie Ma, Konrad Puzniak, Bella Lake, Karin Schmalzl, and Christian Balz designed the experiment. Xiao Wang and Jianda Wu carried out analytical and iTEBD calculation and provided theoretical analysis. Xiao Wang, Konrad Puzniak, Jie Ma, Jianda Wu, and Bella Lake wrote the manuscript.

Appendix A. Supplementary materials

Supplementary materials to this short communication can be found online at https://doi.org/10.1016/j.scib.2024.07.040.

References

[1] Sachdev S. Quantum Phase Transitions. Cambridge, England: Cambridge University Press; 2011. p. 1–521.
[2] Zamolodchikov AB. Integrals of motion and S-Matrix of the (scaled) $T = T_c$ Ising model with magnetic field. Int J Mod Phys A 1989;4:4235.
[3] Pfeuty P. The one-dimensional Ising model with a transverse field. Annalen der Physik 1970;59:79–90.
[4] Boyanovsky D. Field theory of the two-dimensional Ising model: Conformal invariance, order and disorder, and bosonization. Phys Rev B 1989;39:6744.
[5] Zou H, Cui Y, Wang X, et al. E_8 spectra of quasi-one-dimensional antiferromagnet $BaCo_2V_2O_8$ under transverse field. Phys Rev Lett 2021;127:077201.
[6] Wang X, Zou H, Hódsági K, et al. Cascade of singularities in the spin dynamics of a perturbed quantum critical Ising chain. Phys Rev B 2021;103:235117.
[7] Coldea R, Tennant DA, Wheeler EM, et al. Quantum criticality in an Ising chain: Experimental evidence for emergent E_8 symmetry. Science 2010;327:177.
[8] Amelin K, Engelmayer J, Viirok J, et al. Experimental observation of quantum many-body excitations of E_8 symmetry in the Ising chain ferromagnet $CoNb_2O_6$. Phys Rev B 2020;102:104431.
[9] Amelin K, Viirok J, Nagel U, et al. Quantum spin dynamics of quasi-one-dimensional Heisenberg-Ising magnets in a transverse field: Confined spinons, E_8 spectrum, and quantum phase transitions. J Phys A Math Theor 2022;55:484005.
[10] Fava M, Coldea R, Parameswaran SA. Glide symmetry breaking and Ising criticality in the quasi-1D magnet $CoNb_2O_6$. Proc Natl Acad Sci USA 2020;117:25219.
[11] Niesen SK, Kolland G, Seher M, et al. Magnetic phase diagrams, domain switching, and quantum phase transition of the quasi-one-dimensional Ising-like antiferromagnet $BaCo_2V_2O_8$. Phys Rev B 2013;87:224413.
[12] Faure Q, Takayoshi S, Petit S, et al. Topological quantum phase transition in the Ising-like antiferromagnetic spin chain $BaCo_2V_2O_8$. Nat Phys 2018;14:716–22.
[13] Matsuda M, Onishi H, Okutani A, et al. Magnetic structure and dispersion relation of the S=1/2 quasi-one-dimensional Ising-like antiferromagnet $BaCo_2V_2O_8$ in a transverse magnetic field. Phys Rev B 2017;96:024439.
[14] Zhang Z, Amelin K, Wang X, et al. Observation of E_8 particles in an Ising chain antiferromagnet. Phys Rev B 2020;101:220411.

Xiao Wang is currently a Ph.D. candidate in the Condensed Matter Division of Tsung-Dao Lee Institute at Shanghai Jiao Tong University. He obtained his B.S. degree from Donghua University in 2020. His research interest includes conformal field theory and quantum integrable models, along with their applications.

Jianda Wu obtained his Ph.D. degree from Rice University in 2014. He was a postdoctoral researcher at University of California San Diego, from 2014 to 2017, and a guest scientist at the Max Planck Institute for the Physics of Complex Systems from 2017 to 2018. He is currently an associate professor at Shanghai Jiao Tong University. His research interest includes quantum criticality, quantum many-body dynamics, and exact solutions for strongly correlated systems.

Bella Lake received her Ph.D. degree from Oxford University (1997) and held postdoc positions at the University of Toronto, Canada, Oak Ridge National Laboratory, USA and Risoe National Laboratory, Denmark. In 2005, she joined the Hemholtz Zentrum Berlin for Materials and Energy in Germany where she currently heads the Department "Quantum phenomena in novel materials". She also holds a professorship at Technical University Berlin. Her research focuses on the study of magnetism and strongly correlated materials.

Jie Ma received his Ph.D. degree from Iowa State University (2010) and held postdoc positions at the Oak Ridge National Laboratory, USA and University of Tennessee- Knoxville, USA from 2010 to 2015. He is a professor at the School of Physics and Astronomy, Shanghai Jiao Tong University. His research interest includes quantum magnetism and phonon of the strongly correlated materials.